Ninth International Conference on
THIN-WALLED STRUCTURES – ICTWS2023
Sydney, Australia, Nov 29 – Dec 1, 2023

DESIGN OF WELDED STEEL I-SECTION MEMBERS BY GMNIA WITH CSM STRAIN LIMITS

Xiang Yun*, Yufei Zhu,*** and Leroy Gardner****

* Department of Civil and Structural Engineering, The University of Sheffield, Sheffield S1 3JD, UK
e-mail: x.yun@sheffield.ac.uk

** Department of Civil and Environmental Engineering, Imperial College London, London SW7 2AZ, UK
e-mail: yufei.zhu18@imperial.ac.uk, leroy.gardner@imperial.ac.uk

*** School of Civil Engineering, Shanghai Normal University, Shanghai 201418, PRC

Keywords: Advanced analysis; Continuous Strength Method (CSM); GMNIA; High strength steel; Local buckling; Second order effects.

Abstract. *This present study extends the framework of a recently proposed advanced design method which employs computationally efficient beam element models to perform GMNIA and utilises strain limits, defined by the Continuous Strength Method (CSM), to simulate local buckling behaviour in the beam element models to both normal strength and high strength steel (NSS and HSS) welded I-section members. The proposed advanced design method makes a rational allowance for material nonlinearity (i.e. the spread of plasticity and material strain hardening) and takes due account of the influence of moment gradient in the determination of ultimate resistances. The accuracy of the proposed advanced design method for NSS and HSS welded I-section members is evaluated by means of comparisons with a large amount of benchmark numerical data obtained from shell FE models, considering varying steel grades, loading scenarios and cross-section and member slendernesses. Compared to the traditional design approaches set out in the current Eurocode 3 (EC3) provisions, the proposed advanced design method can provide consistently more accurate and safe sided resistance predictions for both NSS and HSS welded I-section members subjected to various loading conditions.*

1 INTRODUCTION

For ease and efficiency in practical design, the structural analysis is commonly conducted using beam finite elements, which cannot capture cross-sectional local buckling behaviour. The cross-sectional local buckling is thus accounted for by means of a cross-section classification framework where cross-sections are generally categorised into several discrete behavioural classes according to their susceptibility to local buckling and rotation capacities, upon which different analysis types and design rules are assigned accordingly [1]. The concept of cross-section classification, however, fails to accurately account for the effects of element interaction, strain hardening and spread of plasticity on the determination of cross-sectional resistances, sometimes leading to rather inaccurate and scattered resistance predictions of members and structural systems. Moreover, plastic design of HSS structures is not permitted in current design standards [],[3] owing to the relatively low ductility and low ultimate-to-yield strength ratio of HSS, while recent studies have shown that this restriction can lead to unduly conservative resistance predictions for HSS structures [],[5]. The shortcomings of existing design methods emphasise the necessity to develop advanced analysis that directly captures various influencing factors including instability, plasticity, residual stresses and initial geometric imperfections within structural elements and systems, thereby allowing for a direct understanding of true structural behaviour.

The focus of this paper is to extend a recently developed framework of design by advanced analysis []-[8] to both NSS and HSS welded I-section members subjected to various loading scenarios. Benchmark shell FE models were firstly developed and validated against existing test data on welded I-section members subjected to bending, compression and combined loading. The validated shell FE models were then employed to generate additional benchmark data which were used to assess the accuracy of the proposed GMNIA + CSM design framework, relative to the conventional Eurocode design methods. The key features of the proposed GMNIA + CSM framework, including the CSM strain limits that define the maximum attainable strain prior to cross-section failure, the strain averaging approach that allows for the influence of moment gradient and the shear resistance check that accounts for the influence of high shear forces, are presented and discussed. The assessments revealed that the proposed GMNIA + CSM design approach offers more accurate and consistent resistance predictions for both NSS and HSS welded I-section members subjected to different loading scenarios compared to the current EC3 design approaches.

2 BENCHMARK SHELL FINITE ELEMENT MODELLING

2.1 Basic modelling assumptions

In this section, shell FE models were developed to generate extensive benchmark data for the assessment of the proposed GMNIA + CSM design framework for NSS and HSS welded I-sections subjected to different loading scenarios. The benchmark shell FE models were created using the four-noded shell element with reduced integration S4R in the FE software ABAQUS [9]. The notation of the geometries of modelled welded I-sections is shown in Figure 1, where B is the flange width, H is the outer section depth, t_f is the flange thickness, t_w is the web thickness, t_{weld} is the weld leg length, b_f is the clear width of the outstand flange equal to $(B-t_w)/2-t_{weld}$, and h_w is the clear height of the web equal to $H-2t_f-2t_{weld}$. The flange width of each modelled I-section was subdivided into an even number of elements with the mesh size approximately equal to $(B+H)/40$. The selected mesh size was also applied along the web depth and the member length, resulting in an element aspect ratio close to unity.

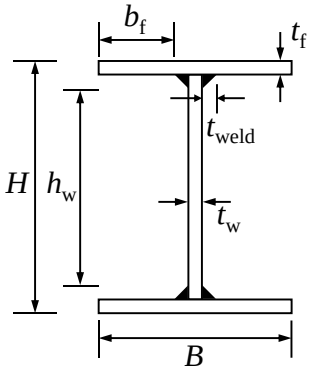

Figure 1: Notation for modelled welded I-sections

Both global and local geometric imperfections were incorporated into each shell FE model by modifying the nodal coordinates of the perfect geometry []-[15]. Global imperfections were assumed in the shape of a half sinusoidal wave with the imperfection magnitude equal to $L/1000$, where L is the member length, and were introduced into the FE models subjected to compression and combined compression and bending. Local imperfections were introduced into the FE models subjected to all types of loading scenarios as a series of sinusoidal waves

with the imperfection magnitude defined following the recommendations given in EN 1993-1-5 [10].

The measured stress-strain curves from previous experimental programmes were used for the validation of the developed shell FE models, while for the subsequent parametric studies, the bilinear plus nonlinear hardening stress-strain model developed by Yun and Gardner [12] for hot-rolled steels was used to generate engineering stress-strain curves for all the steel grades considered in this research. The Poisson's ratio v was taken equal to 0.3 in the elastic range and 0.5 in the plastic range. The engineering stress-strain curves were transformed into true stress-logarithmic plastic strain curves before inputting into the FE models. The residual stress pattern proposed by Yun et al. [13] for welded I-sections with varying steel grades was introduced into the FE models as an initial stress condition. A preliminary analysis step was defined to achieve equilibration of the residual stresses, and a subsequent analysis step was set up for the application of external loadings by means of the modified Riks method, enabling the full load-deformation responses of the FE models to be captured.

Suitable boundary conditions and external loadings were applied at reference points which were coupled with nodes within the corresponding end sections or load regions through rigid body constraints. For members subjected to bending alone, transverse stiffeners were modelled and attached to the cross-sections at which the loading was applied to effectively prevent localised web crippling failure under concentrated transverse force. Note that for members bending/buckling about the major axis, the out-of-plane displacement degree of freedom was restrained along the flange centrelines at adequate intervals to prevent lateral torsional buckling. The same modelling approach has been successfully employed in previous studies, providing reliable numerical simulations [],[14].

2.2 Validation

The developed shell FE models were validated against a total of 48 experimental results on HSS welded I-section members subjected to different loading scenarios, including beams in three- and four-point bending [],[16], columns buckling about the major and the minor axes [],[]-[19] and beam-columns subjected to combined compression and minor axis bending [],[21]. The measured geometries and material properties were used in the shell FE models for validation purposes. Note that the fillet welds of the I-sections were explicitly modelled using five web elements at each web-flange interaction with different increased thicknesses [],[15]. The material properties of the fillet welds, if not available in the literature, were assumed to be equal to those of the web plate.

Comparisons of the numerically obtained ultimate capacities $R_{u,FE}$ against the corresponding test results $R_{u,test}$ are summarised in Table 1, including the mean and coefficient of variation (COV) values of the $R_{u,FE}/R_{u,test}$ ratios for welded I-section members subjected to different loading conditions. It can be seen from Table 1 that the developed shell FE models are able to provide ultimate capacities very close to the corresponding test results. The numerically obtained load-deformation curves also agree well with the corresponding experimental curves, as shown in Figure 2(a) for typical beam specimens and Figure 2(b) for typical column and beam-column specimens. Hence, it can be concluded that the developed shell FE models can accurately simulate the structural response of welded I-section members and are able to provide reliable benchmark data for the assessment of different design approaches as discussed in the following sections.

Table 1: Comparisons of test and numerical results for welded I-section members subjected to different loading scenarios

Member type	Loading scenario	Steel grade	No. of tests	$R_{u,FE}/R_{u,test}$		References
				Mean	COV	
Beam	Three/four-point bending	S690	12	1.02	0.02	[],[16]
Column	Buckling about major axis/minor axis	Q460GJ, S690, Q960	20	0.96	0.07	[],[]-[19]
Beam-column	Compression + minor axis bending	Q460GJ, S690	16	0.98	0.04	[],[21]

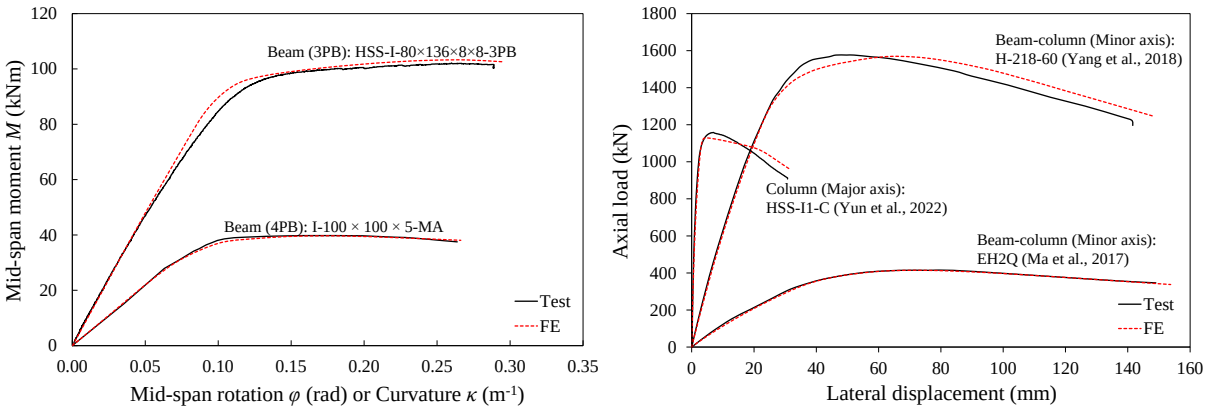

(a) Beams (b) Columns and beam-columns

Figure 2: Comparisons of typical test and FE load-deformation curves for welded I-section beams [],[16], columns [13] and beam-columns [],[21] made of S690 steel.

2.3 Parametric study

Upon validation of the shell FE models, a comprehensive parametric study was performed to create extensive benchmark data for the evaluation of different design approaches. All the modelled welded I-sections in the parametric study had a fixed flange width B of 100 mm, while three outer section depths H of 100 mm, 150 mm, and 200 mm were considered, resulting in cross-section aspect ratios equal to 1.0, 1.5 and 2.0, respectively. Different values of flange and web thicknesses were selected to generate a broad spectrum of cross-section slenderness values $\bar{\lambda}_p$ varying from 0.2 to 1.0 (i.e. covering cross-sections from Class 1 to Class 4 according to prEN 1993-1-1 [22]). For members subjected to bending, the web thickness t_w of each modelled I-section was taken equal to 0.6 times the corresponding flange thickness t_f (i.e. $t_w = 0.6t_f$), which represents a most common web-to-flange thickness ratio for standard hot-rolled UB and IPE profiles. For members subjected to compression or combined loading, the flange and web thicknesses of each modelled I-section were determined such that their corresponding plate slendernesses in compression were approximately equal (i.e. the flange plate slenderness $\bar{\lambda}_{p,f} \approx$ the web plate slenderness $\bar{\lambda}_{p,w}$), thereby minimising the influence of element interaction between the flange and the web on the ultimate resistances of these structural members. Note that the fillet welds of the I-sections were ignored throughout the parametric study. S355 steel and S690 steel welded I-sections were considered in the parametric study. The stress-strain curves of the two adopted steel grades (i.e. S355 and S690) were represented by the bilinear plus nonlinear material model proposed by Yun and Gardner [12]. Key material properties (E, f_y and f_u) of the considered steel grades are provided in Table 2.

Table 2: Key mechanical properties for S355 and S690 steels employed in the present study.

Steel grade	E	f_y	f_u
	N/mm^2	N/mm^2	N/mm^2
S355	210000	355	490
S690	210000	690	770

3 DESIGN BY GMNIA USING BEAM FINITE ELEMENTS WITH STRAIN LIMITS

To overcome the limitations of the current EC3 design approaches, a practical method of design by advanced analysis was proposed by Fieber et al. [],[23] for steel structures. The proposed design method consists of: (1) conducting a GMNIA using beam FE models, and (2) determining the ultimate capacities of individual members or structures in accordance with either the peak load factor or the load factor at which a specific strain limit, defined by the CSM, is attained, whichever occurs first. Extension of this method to HSS prismatic welded I-section members is addressed in this section.

3.1 Continuous Strength Method (CSM)

The Continuous Strength Method (CSM) is a deformation-based method that replaces the concept of cross-section classification with a continuous relationship (i.e. the CSM base curve) between cross-section slenderness $\bar{\lambda}_p$ and deformation capacity (strain ε) [1]. The CSM base curve, given by Eq. (1) for plated cross-sections, defines the limiting strain ε_{csm} that a cross-section can endure prior to local buckling. In Eq. (1), cross-section slenderness $\bar{\lambda}_p$ is equal to the square root of the yield strength f_y divided by the elastic local buckling stress of the cross-section $\sigma_{cr,cs}$, as given by Eq. (2), ε_y is the yield strain equal to the yield strength f_y divided by the Young's modulus E, ε_u is the ultimate strain estimated as $\varepsilon_u = 0.6(1-f_u/f_y)$ but no less than 0.06 for hot-rolled steels [12] where f_u is the ultimate strength and C_1 is a coefficient corresponding to the quad-linear material model developed by Yun and Gardner [12].

$$\frac{\varepsilon_{csm}}{\varepsilon_y} = \begin{cases} \dfrac{0.25}{\bar{\lambda}_p^{3.6}} \le \min\left(\Omega, \dfrac{C_1\varepsilon_u}{\varepsilon_y}\right) & \text{for } \bar{\lambda}_p \le 0.68 \\ \left(1-\dfrac{0.222}{\bar{\lambda}_p^{1.05}}\right)\dfrac{1}{\bar{\lambda}_p^{1.05}} & \text{for } \bar{\lambda}_p > 0.68 \end{cases} \tag{1}$$

$$\bar{\lambda}_p = \sqrt{\frac{f_y}{\sigma_{cr,cs}}} \tag{2}$$

Two upper bounds are imposed on the strain ratio $\varepsilon_{csm}/\varepsilon_y$ of Eq. (1). The first limit of Ω is set to prevent excessive strains and defines the acceptable level of plastic deformation, which is determined on a project-specific basis. As per the ductility requirement outlined in EN 1993-1-1 [22], a generally recommended value of 15 is proposed. The second limit of $C_1\varepsilon_u/\varepsilon_y$ defines a cut-off strain to prevent over-predictions of material strength [],[],[24]. Experimental investigations []-[27] revealed that certain I-section beams made of HSS experienced brittle fractures on their flange plates under tension, with a fracture strain ε_f of approximately 7-8% (equivalent to $\varepsilon_f/\varepsilon_y$ = 15-18). Consequently, it is advised to set a value of Ω = 10 as the upper limit for the CSM base curve when designing HSS structures. This limitation helps avoid the

undesirable occurrence of brittle fracture on tensile plate elements made of HSS before reaching design loads. To conclude, the present study considers values of $\Omega = 15$ for the design of NSS structures and $\Omega = 10$ for the design of HSS structures.

3.2 Implementation of CSM strain limit to GMNIA using beam finite elements

The proposed design method is implemented by initially conducting GMNIA using beam finite elements. In this study, beam FE models were established using the ABAQUS software [9]. It should be noted that this method can also be applied in other structural analysis software capable of fully capturing material nonlinearity and second-order effects at the member and system levels (i.e. $P - \delta$ and $P - \Delta$ effects).

For the beam FE models, a 2-noded shear deformable Timoshenko beam element for open sections (B31OS in the ABAQUS element library) was employed. To ensure accurate simulation of the spread of plasticity through the cross-section and the distribution of initial residual stresses, a total of 121 section points were assigned to the full cross-section. The incorporation of residual stresses into the beam FE models was achieved by defining the initial stress values at the section points using the SIGINI user subroutine [28]. Additionally, global geometric imperfections were introduced through a half sinusoidal wave shape with a magnitude equal to $L/1000$, and nodal coordinates were adjusted from the perfect geometry to model these imperfections.

The mesh size of each beam FE model was set equal to that used in the longitudinal direction of the corresponding shell FE model, with a requirement that the selected mesh sizes should not exceed the relevant local buckling half-wavelength $L_{b,cs}$ of the modelled cross-section to apply the strain averaging approach effectively [6]. The true stress-logarithmic plastic strain curves based on the bilinear plus nonlinear hardening material model [12] was input into the beam FE models. Suitable boundary conditions were applied to the beam FE models, while for welded I-section columns buckling about the major axis and beams bending about the major axis, lateral torsional buckling was effectively prevented by employing appropriate lateral restraints. The validity of the developed beam FE models under different loading conditions was confirmed by comparing load-deformation and load-strain histories obtained from the beam FE models against those from the benchmark shell FE models.

Upon conducting GMNIA using beam finite elements, the ultimate capacity of an individual member can be determined through the following procedure:

(1) The elastic local buckling stress $\sigma_{cr,cs}$ and the local buckling half-wavelength $L_{b,cs}$ for the constituent cross-section are calculated using the analytical formulae from [29], considering the first-order internal force and moment distribution along the member. The cross-section slenderness $\bar{\lambda}_p$ is then obtained based on the elastic local buckling stress $\sigma_{cr,cs}$ using Eq. (2). The CSM limiting strain ε_{csm} is determined based on the cross-section slenderness $\bar{\lambda}_p$ using Eq. (1).

(2) In the case of a member subjected to a moment gradient, the strain averaging approach [6] should be applied, and the averaged compressive strain outputs $\varepsilon_{Ed,av}$ are checked against the CSM limiting strain ε_{csm}. Otherwise, for members without a moment gradient, the maximum compressive strain outputs $\varepsilon_{Ed,max}$ are checked against the CSM limiting strain ε_{csm}. Note that in all cases considered in this study, the compressive strain outputs and the corresponding CSM limiting strain are both compatibly determined at the centreline of the wall thickness, following the suggestion by Fieber et al. [6].

(3) Finally, the ultimate capacity of the member is determined based on either the peak load factor α_{peak} or the CSM load factor α_{csm}, whichever is occurred first. If the peak load factor α_{peak} is reached first, the ultimate capacity is considered equal to the peak load; otherwise, if the CSM load factor α_{csm} is attained first, the ultimate capacity is defined by the load at which the CSM limiting strain is reached.

4 EVALUATION OF THE PROPOSED DESIGN METHOD

The accuracy of the proposed advanced design method for HSS welded I-section members subjected to bending, compression, and combined compression with uniaxial bending is assessed in this section. Comparisons are made against the current EC3 design approaches. The assessment was carried out by comparing the benchmark shell FE results R_{shell} against the ultimate capacities predicted using the advanced design method R_{pred}. Note that a value of R_{shell}/R_{pred} greater than 1.0 indicates a conservative resistance prediction by the proposed advanced design method, while a value less than 1.0 implies an unconservative prediction.

4.1. Members subjected to bending

To assess the accuracy of the proposed advanced method for designing HSS welded I-section members subjected to major-axis bending, a comprehensive analysis was conducted on a total of 400 simply supported welded I-section beams made of S355 and S690 steel. These beams were subjected to loading under three- or four-point bending, with varying local cross-section slenderness.

The normalised bending moment capacities ($M_{u,FE}/M_{el,y}$) derived from the FE models for all S690 steel welded I-section beams subjected to three-point bending are plotted in Figure 3, in which $M_{el,y}$ is the elastic moment capacities about the major axis, defined as the product of the major axis elastic section modulus $W_{el,y}$ and the yield stress f_y. Additionally, moving averages over 5 adjacent data points of the benchmark shell FE results and the predicted results obtained using the proposed advanced design method are also presented in the figure. For Class 3 cross-sections, the resistances can alternatively be determined from elasto-plastic bending moment capacities M_{ep}, which are defined as the product of the elasto-plastic section modulus W_{ep} and the yield stress f_y, where W_{ep} is linearly interpolated between W_{el} and the plastic section modulus W_{pl}. The proposed design method, employing an upper limit of $\Omega = 15$ for NSS and $\Omega = 10$ for HSS, generally yields more accurate and consistent bending moment resistance predictions compared to the EC3 design rules. Notably, for HSS cross-sections with $\bar{\lambda}_p \leq 0.36$, the proposed design method, utilising the upper limit of $\Omega = 15$, provides highly accurate resistance predictions, while employing the upper limit value $\Omega = 10$ results in more conservated predictions. Therefore, considering the lower ductility, the value of 10 is recommended for HSS design. The proposed advanced design method provides slightly conservative resistance predictions for HSS welded I-section 3-point bending beams with $\bar{\lambda}_p > 0.68$ (i.e. Class 4 cross-sections). This behaviour is primarily attributed to the fundamental CSM base curve, which predicts the relationship between strain ratio and slenderness more conservative for slender cross-sections compared to non-slender cross-sections [1].

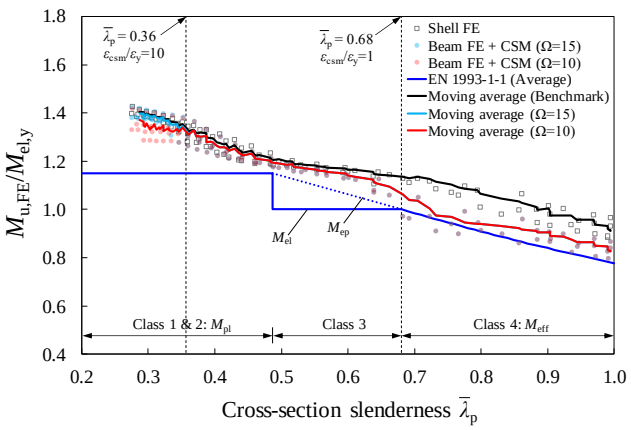

Figure 3: Bending resistance predictions for homogeneous S690 steel welded I-sections of varying slenderness under major-axis three-point bending (with moving averages over 5 adjacent data points).

A statistical analysis was conducted on the ratios of the benchmark shell FE results to the bending moment resistance predictions obtained using the advanced design method (i.e. $M_{u,shell}/M_{pred}$). The results indicated that the current EC3 design rules tend to be conservative for both NSS and HSS, with overall mean and COV values of $M_{u,shell}/M_{pred}$ equal to 1.087 and 0.075, respectively. However, the proposed advanced design with an upper limit of $\Omega = 15$ for NSS and $\Omega = 10$ for HSS showed improved accuracy and consistency in resistance predictions, with overall mean and COV values of $M_{u,shell}/M_{pred}$ equal to 1.038 and 0.063, respectively.

4.2. Members subjected to compression

To assess the accuracy of the proposed advanced method for the design of HSS welded I-section members subjected to compression, a comprehensive analysis was conducted on a total of 426 pin-ended welded I-section columns made of grade S355 and S690 steel. The analysis considered both major and minor axis buckling, three values of non-dimensional member slenderness ($\overline{\lambda}$ = 0.5, 1.1, 1.7) and varying cross-section slenderness values $\overline{\lambda}_p$ ranging from 0.2 to 1.0. The ultimate buckling capacities obtained from the benchmark shell FE results, the proposed advanced design method, and the current EC3 design approach were all normalised by the plastic squash load N_{pl}, which is the product of the gross cross-section area A and the yield stress f_y. The normalized capacities were then plotted against the cross-section slenderness $\overline{\lambda}_p$ in Figure 4.

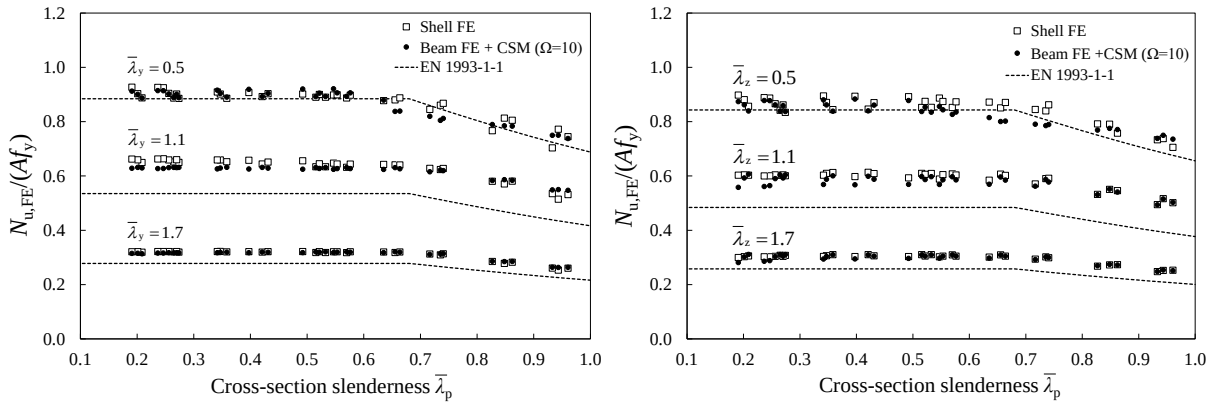

(a) Major axis buckling (b) Minor axis buckling

Figure 4: Resistance predictions of S690 steel welded I-section columns with varying cross-section slenderness $\overline{\lambda}_p$ buckling about (a) the major axis and (b) the minor axis for three values of member slenderness ($\overline{\lambda}$ = 0.5, 1.1, 1.7).

Note that for columns with slender cross-sections (e.g. $\overline{\lambda}_p > 0.6$), the resistance predictions obtained from the proposed advanced design method were primarily governed by the attainment of the CSM strain limit; conversely, for columns with less slender cross-sections (e.g. $\overline{\lambda}_p < 0.6$), the resistance predictions were generally governed by the peak load factors. A statistical analysis of the ratios of $N_{u,shell}/N_{pred}$ for all the considered design methods was conducted. The overall mean and COV values of $N_{u,shell}/N_{pred}$ were respectively equal to 1.016 and 0.030 for the proposed advanced design method, while they were found to be 1.106 and 0.081, respectively, for the current EC3 design approach. Based on the results, it can be concluded that the proposed design method generally provides more accurate and less scattered resistance predictions compared to the current EC3 design approach.

4.3. Members subjected to combined compression and uniaxial bending

In this section, the accuracy of the proposed method for the in-plane stability design of HSS welded I-section members is examined. The analysis included 3960 pin-ended beam-columns subjected to combined compression and uniaxial bending. Both major and minor axis buckling were considered, and the study encompassed three values of member slenderness ($\bar{\lambda}$ = 0.5, 1.1, 1.7) and three bending moment distributions along the member length (ψ = 1.0, 0, -0.5). To achieve different bending moment distributions ψ, the ratio of the applied moments at the column ends (i.e. M_2/M_1) was adjusted, where ψ = 1.0 represents a uniformly distributed bending moment, ψ = 0 corresponds to a linearly distributed bending moment, and ψ = -0.5 denotes a linearly distributed bending moment with $M_2 = -0.5M_1$. Twelve different cross-section sizes of varying local slenderness were considered for each steel grade. The ratio of applied compression to bending was varied to cover the full range of loading scenarios from pure compression to pure bending.

Figure 5 illustrates the normalised moment-compression (*M*-*N*) interaction relationships for a representative series of S690 steel beam-columns subjected to combined compression and uniaxial bending with ψ = 1.0. In the figure, the benchmark shell FE results are compared against the ultimate capacities predicted using three different design methods: (1) the EC3 member buckling checks, (2) linear interaction cross-section checks based on results of second-order elastic analyses (i.e. beam element GNIA + EC3 cross-section checks), and (3) the proposed advanced design method (i.e. beam element GMNIA + CSM strain limits). For predicting the resistances of members with Class 3 cross-sections using the two EC3 design methods, the elasto-plastic section moduli were employed, following the guidelines specified in prEN 1993-1-1 [22]. The GNIA incorporated the elastic reference equivalent bow imperfections as defined in prEN 1993-1-1 [22], which are equal to *L*/110 for members buckling about the major axis and equal to *L*/200 for members buckling about the minor axis, where *L* is the member length.

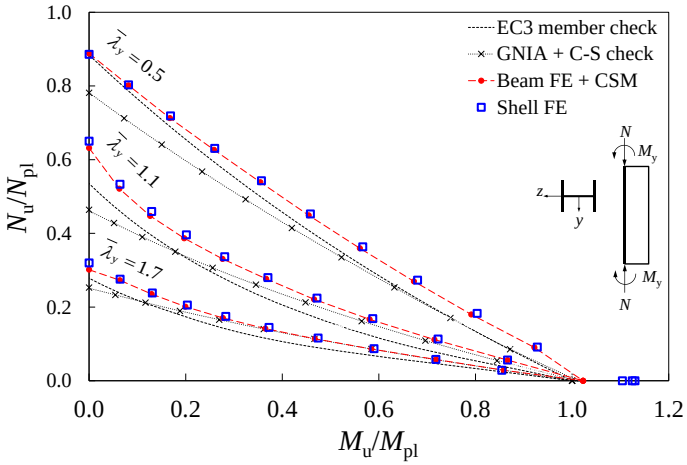

Figure 5: Comparison of the benchmark shell FE results against the ultimate capacities predicted using different design methods for S690 steel pin-ended beam-columns with different member slenderness and ψ = 1.0 under combined compression plus major axis bending (Class 1 welded I-section: 100 × 100 × 16 × 7.8 in mm, $\bar{\lambda}_p$ = 0.27 in compression).

The comparisons demonstrate that the two EC3 design methods tend to yield slightly more conservative resistance predictions for members subjected to compression plus uniform bending (i.e. ψ = 1), and somewhat imprecise, yet generally safe-sided, resistance predictions for members subjected to compression plus non-uniform bending (i.e. ψ = 0 and ψ = -0.5). In contrast, the proposed advanced design method provides resistance predictions that are

generally safe-sided and closely aligned with the benchmark shell FE results. It is worth noting that, in the proposed advanced design method, resistance predictions for short members and cases dominated by bending are primarily governed by the CSM load factor α_{csm}, while for longer members and cases dominated by compression, the resistance predictions were generally governed by the peak load factors α_{peak}.

A statistical analysis was conducted on the ratios of R_{shell}/R_{pred} for all the considered design methods, where R_{shell} and R_{pred} represent the radial distances measured from the origin to the datapoint of the benchmark shell FE results and the datapoint predicted using the considered design method, respectively, in the normalized N-M interaction diagram, as illustrated in Figure 6. Overall, the proposed advanced design method provides the most accurate, yet still generally safe-sided, resistance predictions for both NSS and HSS welded I-section beam-columns, with the overall mean and COV values of R_{shell}/R_{pred} equal to 1.031 and 0.053, respectively. In contrast, the resistance predictions offered by the two EC3 design approaches exhibit greater scatter and conservatism, particularly for bending-dominated cases. The overall mean and COV values of R_{shell}/R_{pred} are equal to 1.124 and 0.132, respectively, for the EC3 member buckling checks, and equal to 1.130 and 0.128, respectively, for the approach of the linear interaction cross-section checks using GNIA.

The significant advantages of the proposed advanced design method over the current EC3 design approaches arise from the following aspects: (1) accounting for the interaction between flange and web plates in the determination of cross-section local slenderness $\bar{\lambda}_p$, (2) rational utilisation of the beneficial effects of material strain hardening and local moment gradients in the determination of ultimate capacities through the use of more precise material models and the application of the strain averaging approach, (3) direct capture of second-order effects and the spread of plasticity in the GMNIA analysis, and (4) elimination of the need for separate member checks (including the calculation of effective lengths and moment gradient factors) as well as the calculation of effective section moduli W_{eff} for Class 4 cross-sections.

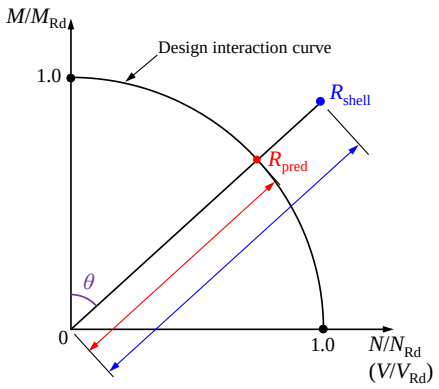

Figure 6: Definition of radial distances *R* in normalised *M-N* interaction diagram.

5 CONCLUSIONS

This paper presents a recently proposed advanced design framework for both NSS and HSS welded I-section structural members subjected to various loading scenarios. The framework utilises computationally efficient beam element models to conduct GMNIA and incorporates strain limits defined by the Continuous Strength Method (CSM) to simulate local buckling behaviour. Shell FE models were created and validated against existing test data on welded I-section structural members, and subsequently used in a comprehensive parametric study to generate benchmark FE results for the assessment of the proposed advanced design method,

considering a broad range of cross-section slendernesses, member slendernesses and different loading conditions. The assessment demonstrated that the proposed advanced design method, with an upper CSM strain ratio limit of $\Omega = 15$ for NSS and $\Omega = 10$ for HSS, consistently provides more accurate resistance predictions compared to the current EC3 design method specified in EN 1993-1-1 [22]. Further research is currently underway to extend this practical advanced design approach to structural steel indeterminate structures.

REFERENCES

[1] Gardner L., Yun X., Walport F., "The Continuous Strength Method – Review and outlook", *Engineering Structures*, **275**, 114924, 2023.

[2] EN 1993-1-12:2007. Eurocode 3: Design of steel structures – Part 1-12: Additional rules for the extension of EN 1993 up to steel grades S700. European Committee for Standardization (CEN), Brussels; 2007.

[3] ANSI/AISC 360-16. Specification for Structural Steel Buildings, American Institute of Steel Construction (AISC), Chicago, Illinois, 2016.

[4] Gkantou M., Theofanous M. and Baniotopoulos C., "Plastic design of hot-finished high strength steel continuous beams", *Thin-Walled Structures*, **133**, 85-95, 2018.

[5] Yun X., Zhu Y., Wang Z. and Gardner L., "Benchmark tests on high strength steel frames", *Engineering Structures*, **258**, 114108, 2022.

[6] Fieber A., Gardner L. and Macorini L., "Design of structural steel members by advanced inelastic analysis with strain limits", *Engineering Structures*, **199**, 109624, 2019.

[7] Quan C., Kucukler M. and Gardner L., "Design of web-tapered steel I-section members by second-order inelastic analysis with strain limits", *Engineering Structures*, **224**, 111242, 2020.

[8] Walport F., Gardner L., Nethercot D.A., "Design of structural stainless steel members by second order inelastic analysis with CSM strain limits", *Thin-Walled Structures*, **159**, 107267, 2021.

[9] Abaqus 2018. SIMULIA - Dassault Systèmes; 2018.

[10] EN 1993-1-5:2006. Eurocode 3: Design of steel structures – Part 1-5: Plated structural elements. European Committee for Standardization (CEN), Brussels; 2006.

[11] Fieber A., Gardner L. and Macorini L., "Formulae for determining elastic local buckling half-wavelengths of structural steel cross-sections", *Journal of Constructional Steel Research*, **159**, 493–506, 2019.

[12] Yun X. and Gardner L., "Stress-strain curves for hot-rolled steels", *Journal of Constructional Steel Research*, **133**, 36–46, 2017.

[13] Yun X., Zhu YF., Meng X. and Gardner L., "Welded steel I-section columns: Residual stresses, testing, simulation and design", *Engineering Structures*, **282**, 115631, 2023.

[14] Zhu YF., Yun X. and Gardner L., "Numerical modelling and design of normal and high strength steel non-slender welded I-section beam-columns", *Thin-walled Structures*, **186**, 110654, 2023.

[15] Zhu YF., Yun X. and Gardner L., "Behaviour and design of high strength steel homogeneous and hybrid welded I-section beams", *Engineering Structures*, **275**, 115275, 2023.

[16] Sun Y., He A., Liang YT. and Zhao O., "In-plane bending behaviour and capacities of S690 high strength steel welded I-section beams", *Journal of Constructional Steel Research*, **162**, 105741, 2019.

[17] Deng Y., Zhou S., Li J., Nie S. and Liu P., "Buckling behaviour of Q460GJ welded H-section columns subjected to minor axis under axial compression", *Structures*, **34**, 1416-1428, 2021.

[18] Ban H., Shi G., Shi Y. and Bradford MA., "Experimental investigation of the overall buckling behaviour of 960 MPa high strength steel columns", *Journal of Constructional Steel Research*, **88**, 256-266, 2013.

[19] Li TJ., Li GQ., Chan SL. and Wang YB., "Behavior of Q690 high-strength steel columns: Part 1: Experimental investigation", *Journal of Constructional Steel Research*, **123**, 18-30, 2016.

[20] Yang B., Shen L., Kang SB., Elchalakani M. and Nie SD., "Load bearing capacity of welded Q460GJ steel H-columns under eccentric compression", *Journal of Constructional Steel Research*, **143**, 320-330, 2018.

[21] Ma TY., Hu YF., Liu X., Li GQ. and Chung KF., "Experimental investigation into high strength Q690 steel welded H-sections under combined compression and bending", *Journal of Constructional Steel Research*, **138**, 449-462, 2017.

[22] prEN 1993-1-1:2018. Eurocode 3: Design of steel structures – Part 1-1: General rules and rules for buildings. European Committee for Standardization (CEN), Brussels; 2018. Final document.

[23] Fieber A., Gardner L. and Macorini L., "Structural steel design using second-order inelastic analysis with strain limits", *Journal of Constructional Steel Research*, **168**, 105980, 2020.

[24] Yun X., Gardner L. and Boissonnade N., "The continuous strength method for the design of hot-rolled steel cross-sections", *Engineering Structures*, **157**, 179–191, 2018.

[25] Lee C-H., Han K-H., Uang C-M., Kim D-K., Park C-H., Kim J-H., et al., "Flexural Strength and Rotation Capacity of I-Shaped Beams Fabricated from 800-MPa Steel", *Journal of Structural Engineering*, **139**, 1043–1058, 2013.

[26] McDermott JF., "Plastic Bending of A514 Steel Beams", *Journal of the Structural Division*, **95**, 1851–1871, 1969.

[27] Ricles JM., Sause R. and Green PS., "High-strength steel: Implications of material and geometric characteristics on inelastic flexural behaviour", *Engineering Structures*, **20**, 323–335, 1998.

[28] Abaqus. ABAQUS/standard user's manual, version 6.17. Dassault Systèmes Simulia Corp, USA; 2017.

[29] Gardner L., Fieber A. and Macorini L., "Formulae for Calculating Elastic Local Buckling Stresses of Full Structural Cross-sections", *Structures*, **17**, 2–20, 2019.